

Prognostic impact of T2-weighted CMR imaging for cardiac amyloidosis

Ralf Wassmuth · Hassan Abdel-Aty · Steffen Bohl · Jeanette Schulz-Menger

Received: 2 November 2010 / Revised: 31 January 2011 / Accepted: 2 February 2011 / Published online: 29 March 2011
© European Society of Radiology 2011

Abstract

Objectives Using cardiac magnetic resonance imaging (MRI) we tested the diagnostic value of various markers for amyloid infiltration.

Methods We performed MRI at 1.5 T in 36 consecutive patients with cardiac amyloidosis and 48 healthy volunteers. The protocol included cine imaging, T2-weighted spin echo, T1-weighted spin echo before and early after contrast and late gadolinium enhancement. We compared the frequency of abnormalities and their relation to mortality.

Results Median follow-up was 31 months. Twenty-three patients died. Mean left ventricular (LV) mass was 205 ± 70 g. LV ejection fraction (EF) was $55 \pm 12\%$. T2 ratio was 1.5 ± 0.4 . 33/36 patients had pericardial and 22/36 had pleural effusions. All but two had heterogeneous late enhancement. Surviving patients did not differ from those who had died with regard to gender, LV mass or volume. Surviving patients had a significantly higher LVEF ($60.4 \pm 9.9\%$ vs. $51.6 \pm 11.5\%$; $p=0.03$). The deceased patients had a lower T2 ratio than those who survived (1.38 ± 0.42 vs. 1.76 ± 0.17 ; $p=0.005$). Low T2 was associated with shorter survival (Chi-squared 11.3; $p<0.001$). Cox regression

analysis confirmed T2 ratio <1.5 as the only independent predictors for survival.

Conclusion Cardiac amyloidosis is associated with hypointense signal on T2-weighted images. A lower T2 ratio was independently associated with shortened survival.

Keywords Magnetic resonance imaging · Cardiac · Amyloidosis · Contrast · T2

Introduction

In patients with amyloidosis, myocardial involvement severely affects the prognosis [1, 2], but often remains clinically undetected [3]. Non-invasive diagnosis of cardiac amyloidosis is usually based on left ventricular (LV) hypertrophy in the absence of other causes combined with low voltage on electrocardiography (ECG) [4]. However, it is often challenging to differentiate clinically between various forms of ventricular hypertrophy, e.g. amyloidosis versus hypertrophic cardiomyopathy or advanced hypertensive heart disease [5]. Low voltage ECG has a limited sensitivity and specificity as a marker for cardiac amyloidosis [6]. The sensitivity of a “typical” sparkling pattern on echocardiography to detect amyloidosis was recently found to be as low as 26% [4]. Novel biological markers for heart failure like troponin or B-type natriuretic peptide add benefit but remain unspecific on their own [7–9]. Cardiac magnetic resonance imaging (CMR) provides the ability to visualise LV mass, function and tissue composition within one examination. Late gadolinium enhancement (LGE) can be used to detect a spectrum of myocardial injuries and readily differentiates between myocardial infarction [10] and numerous non-ischaemic cardiomyopathies [11–15]. Yet another intrigu-

R. Wassmuth (✉) · H. Abdel-Aty · S. Bohl · J. Schulz-Menger
HELIOS Klinikum Berlin Buch & Charite Campus Buch,
Schwanebecker Chaussee 50,
13125 Berlin, Germany
e-mail: ralf.wassmuth@charite.de

H. Abdel-Aty
Cardio Imaging Center Berlin,
Berlin, Germany

S. Bohl
Unfallkrankenhaus Berlin,
Berlin, Germany

ing pattern of LGE has recently been reported in patients with cardiac amyloidosis [16–19], which has been linked to altered gadolinium kinetics due to extracellular amyloid deposition. However, in clinical routine this pattern may present with high variability, therefore explaining the interest in additional CMR markers for cardiac amyloidosis. The aim of our study was therefore threefold: firstly, to evaluate the frequency of conventional markers in a large group of amyloidosis patients; secondly, to test the additional value of T2-weighted imaging and early contrast enhancement in T1-weighted CMR for cardiac amyloid infiltration; and finally, to investigate their prognostic impact.

Materials and methods

Patients

We examined 36 consecutive patients (mean age 63 years, range 39–77 years, 19 male, 17 female, all Caucasian) with evidence of cardiac amyloidosis after written and informed consent had been obtained. The local ethical committee approved the study. The patients had heart failure of New York Heart Association class 2.1 ± 0.9 . Echocardiography reports, ECG recordings and chart records were reviewed for evidence of systemic and cardiac amyloidosis.

Eleven patients had amyloidosis-positive myocardial biopsy (Fig. 1) or autopsy. All others had amyloidosis-positive extra-cardiac biopsy plus hypertrophy on echocardiography in the absence of hypertension and peripheral low voltage ECG (amplitude < 0.5 mV). Based on histology 31 patients were diagnosed with AL amyloidosis, two with AA amyloidosis, two with TTR amyloidosis and a single case of senile amyloidosis.

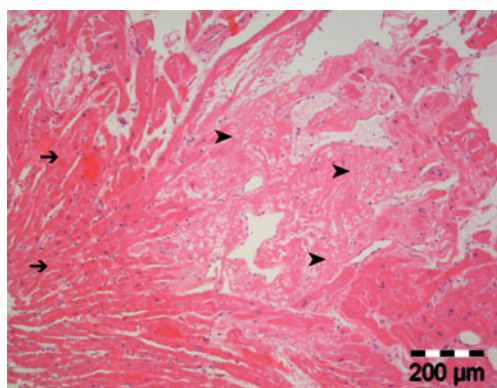


Fig. 1 Light microscopy of HE-stained right ventricular myocardial biopsy specimen reveals eosinophilic amyloid infiltration in patient #19 with AL amyloidosis. Arrows on the left indicate regular myocardial tissue, arrow heads on the right indicate interstitial amyloid infiltration

Survival during follow-up was confirmed by chart review and contact with the referring physician.

Volunteers

Cardiac MRI patient data were compared with reference values derived from 48 healthy subjects (mean age 40 years, median age 42 years, range 18–66 years, 21 male, 19 female) examined after informed consent on a volunteer protocol approved by the local ethics committee. All subjects had an unremarkable medical history and a normal 12-lead ECG.

CMR protocol

Cardiac MRI was performed on clinical one of two 1.5 Tesla MR systems (Siemens Medical Solutions, Erlangen, Germany, or CV/i General Electric Health Care, Waukesha, WI, USA). The same imaging protocol was performed in both patients and volunteers and included the following techniques/pulse sequences:

- 1) LV mass and function: Balanced steady-state free precession (SSFP) gradient echo cine loops were acquired in a two-chamber view (2CV) and a four-chamber view (4CV). Parameters on the Siemens MR system were TR 2.9 ms, TE 1.2 ms, flip angle 80, matrix 256×146 . On the GE MR system TR was 3.8 ms, TE 1.6 ms, flip angle 45, matrix 256×192 . Slice thickness was 8 mm on both systems.
- 2) T2-weighted imaging: Triple-inverted fast spin echo images were acquired in short axis orientation (TR = 2RR, TE = 64 ms, TI = 150 ms, slice thickness 15 mm) using the body coil [20].
- 3) Early gadolinium enhancement: Axial T1-weighted fast spin echo images (TR = 2RR intervals) were obtained before and over the first 4 min immediately after administration of 0.1 mmol/kg Gadolinium-DTPA (Magnevist, Bayer Schering Pharma AG Berlin, Germany). The body coil was used for signal acquisition [21].
- 4) Late gadolinium enhancement (LGE): After testing different inversion times (180–350 ms) for optimal suppression of the myocardium, contiguous stacks of long- and short-axis DE inversion recovery-prepared fast low angle shot gradient echo images were obtained 10–15 min after administration of a second bolus of contrast agent (0.1 mmol/kg) [10]. On the Siemens scanner TR was 11 ms, TE 4.3 ms, flip angle 30, on the GE scanner TR 5 ms, TE 1 ms, flip angle 15. Slice thickness was 8 mm on long axis and 10 mm on short axis images.

Table 1 Quantitative CMR results in patients and volunteers

	Patients (n=36)	Volunteers (n=48)	P value
LVEDVI (ml/m ²)	68±19	82±14	<0.001
LVEF (%)	55±12	61±5	<0.02
LVMI (g/m ²)	111±36	71±12	<0.001
LA area, biplanar (cm ²)	26.5±6.8	22.2±4.4	<0.001
RA area 4CV (cm ²)	24.5±6.6	22.7±4.7	n.s.
Atrial septal thickness (mm)	6±2	5±2	n.s.
RA wall thickness (mm)	4±1	4±1	n.s.
T2 ratio	1.5±0.4	1.7±0.2	<0.05
Early enhancement	7.6±3.2	3.1±1.1	<0.001

n.s., not significant; LVEDVI, left ventricular end-diastolic volume index; LVEF, left ventricular ejection fraction; LVMI, left ventricular mass index; LA, left atrium; RA, right atrium; 4 CV, four-chamber view

Image analysis

Image analysis was done on a satellite workstation of each MR system.

- 1) LV mass and function: One investigator with 13 years of CMR experience manually drew left ventricular contours on end-diastolic and end-systolic cine frames for both 2CV and 4CV. LV volume and mass were calculated and standardised for body surface area. LV ejection fraction (EF) was calculated. To assess atrial size in a time-efficient and pragmatic way the right atrial area was measured in 4CV, the left atrial area (including the left atrial appendage) was measured in 2CV and 4CV and then averaged, as suggested by Anderson et al. [22]. Maximal thickness of the atrial septum and the right atrial free wall were measured.
- 2) T2-weighted imaging: Two independent observers measured signal intensity in a region of interest covering the whole myocardial ring on the short axis and compared it with the signal of the skeletal muscle in the same slice, as previously described [20]. Noise was assessed as the standard deviation of the signal outside the body.
- 3) Early gadolinium enhancement: On T1-weighted fast spin echo images we drew regions of interest covering the myocardium and skeletal muscle in the same slice. Early contrast enhancement was calculated as the ratio of myocardial and skeletal muscle uptake. Values

exceeding the 95% confidence interval in the volunteers were considered abnormal [21].

- 4) Late gadolinium enhancement: Two independent observers visually analysed LGE images for the presence of focal or diffuse hyperintense myocardial lesions, especially for bright subendocardial rims in the left ventricle and the atria. If lesions were definable, the distribution pattern was classified as subendocardial, intramural, transmural or a combination of this. If no focal lesions could be distinguished, but the myocardium could still not be nulled, the pattern was called diffuse.

Statistical analysis

The statistical analysis was performed using SAS 9.2 (SAS Institute Inc., Cary, NC, USA). Results were expressed as mean ± standard deviation and compared with data in the volunteers using Student's t-test after testing for normal distribution. The survival times were displayed as median with interquartile range. Cox regression was used to evaluate whether the factors age, gender, BSA, left atrium (LA) area, right atrium (RA) area, atrial septal thickness, RA wall thickness, left ventricular end-diastolic volume index (LVEDVI), left ventricular mass index (LVMI), EF, T2-signal, early contrast enhancement, presence of pleural or pericardial effusions had an effect on survival. A log-linear model with Weibull distribution for extreme cases

Table 2 Frequency of CMR findings

	Amyloid Patients n (%)	Volunteers n (%)
Abnormal late enhancement	29/31 (94)	0/48 (0)
Pericardial effusion	33/36 (92)	0/48 (0)
Increased early enhancement	28/31 (90)	2/48 (4)
LV hypertrophy	26/36 (72)	0/48 (0)
Pleural effusion	22/36 (61)	0/48 (0)
Left atrial enlargement	20/36 (56)	0/48 (0)

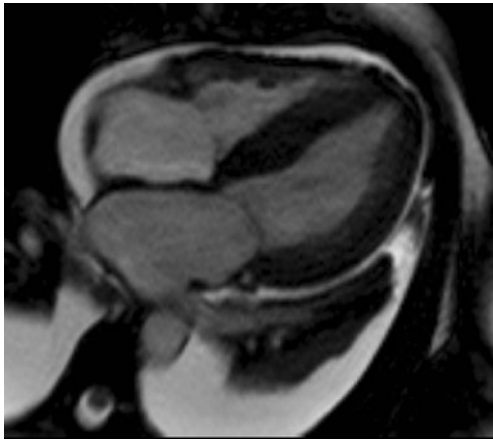


Fig. 2 SSFP cine four-chamber view in diastole illustrating LV hypertrophy, atrial enlargement, pleural and pericardial effusions in a 57-year-old patient

was used to fit the survival model. In a first step, each factor was evaluated independently to assess the significance. Then all factors with p values less than 0.05 were included in an overall model. The final model was chosen by backward selection using a level of significance of 0.05. For further analysis, the continuous variables were dichotomised using the median. For the respective groups, the median survival was estimated from Kaplan-Meier curves. Wilcoxon tests were used to evaluate differences between the groups. No imputations for missing values were performed.

Results

In the volunteer group CMR imaging did not detect any cardiac abnormalities apart from two subjects with increased early enhancement.

Twenty-three patients (64%) died during follow-up in a median time of 4 months after CMR. As assessed clinically death was sudden or due to advanced heart failure in all cases. The surviving patients were followed for 32 ± 17 months (median 31 months, range 8–64). Surviving patients did not differ from those who had died, in gender, LV mass or LV volume. There was a trend towards more advanced age in those who had died ($p=0.048$).

LV mass and function

Quantitative results in patients and controls are summarised in Table 1 and 2. In patients, LV mass index was higher than in volunteers (Fig. 2; 111 ± 36 vs. 71 ± 12 g/m^2 , $p < 0.001$) and exceeded normal values [23] in 26/36 patients (72%). LV volumes were at the lower end of the normal range (68 ± 19 vs. 82 ± 14 ml/m^2 , $p < 0.001$). Left ventricular

ejection fraction (LVEF) varied from normal to reduced (range 27–74%), but was on average still at the lower end of the normal range ($55 \pm 12\%$, compared with $61 \pm 5\%$ in controls, $p < 0.02$). Surviving patients had a significantly

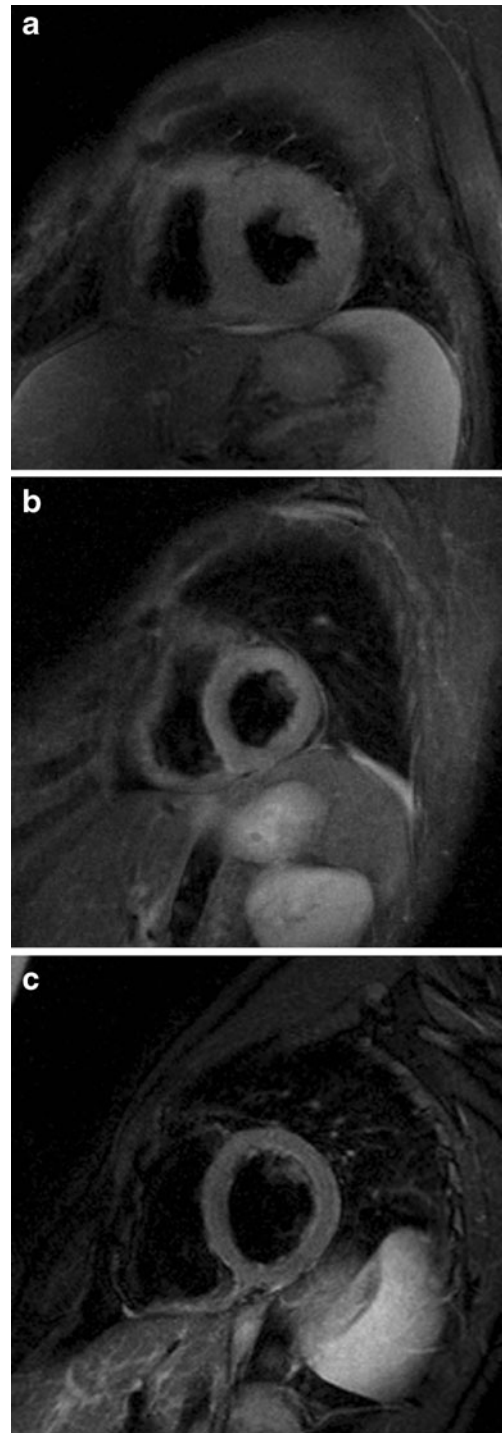


Fig. 3 Triple-inversion T2-weighted fast spin echo imaging on the short axis reveals low myocardial signal intensity in a deceased amyloid patient **a** vs. a surviving amyloidosis patient **b** and a normal volunteer **c**. Window width and level is identical for all 3 figures (275/518)

higher LVEF ($60.4\pm 9.9\%$ vs. $51.6\pm 11.5\%$, $p=0.03$) compared to those who died during follow-up.

The left atrial area was slightly increased in 20/36 (56%) patients ($26.4\pm 6.2\text{ cm}^2$ vs. $23.7\pm 4.4\text{ cm}^2$ in controls, $p<0.001$). Mean right atrial area was at the upper limit of normal with $24.5\pm 6.6\text{ cm}^2$ vs. $22.7\pm 4.7\text{ cm}^2$ in volunteers ($p=0.1$). The maximal thickness of the atrial septum and the mean right atrial free wall thickness did not differ from measurements in healthy controls (6 ± 2 vs. $5\pm 2\text{ mm}$, $p=0.3$; 4 ± 1 vs. $4\pm 1\text{ mm}$, $p=0.9$, respectively).

Small pericardial effusions were present in 33/36 patients (92%), pleural effusions in 22/36 patients (61%; Fig. 2).

T2-weighted imaging

On T2-weighted images myocardial signal intensity indexed to skeletal muscle was lower in patients than in normals (Fig. 3; 1.5 ± 0.4 vs. 1.7 ± 0.2 , $p<0.05$). This was due to a lower myocardial signal intensity in patients (121 ± 55 vs. 151 ± 35 ; $p<0.05$), whereas skeletal muscle signal intensity was not statistically different (82 ± 35 vs. 88 ± 18 ; $p=0.38$). Noise was lower in patients than in volunteers (5.4 ± 2.2 vs. 7.3 ± 1.4 ; $p=0.0001$).

The deceased patients had a lower T2 ratio than those that did survive (Fig. 3; 1.38 ± 0.42 vs. 1.76 ± 0.17 , $p=0.005$). Cox regression analysis confirmed T2 ratio <1.5 signal as the only independent parameter to predict survival (Chi-squared 9.3; $p<0.005$). Kaplan-Meier analysis confirmed the relation between shortened survival and low T2 (Chi-squared 11.3; $p<0.001$).

Early myocardial contrast enhancement

Early myocardial contrast enhancement (Fig. 4) was markedly increased in patients compared with volunteers (mean 7.6 ± 3.2 vs. 3.1 ± 1.1 , $p<0.01$) and exceeded the upper limit of normal in 28/31 patients (90%, non-diagnostic in two, not obtained in three).

LGE imaging

Late gadolinium enhanced images could be obtained in 31/36 patients. In 29 of 31 patients (94%) the myocardial signal could not be suppressed sufficiently, but instead appeared heterogeneous across the range of commonly used inversion times (Fig. 5a). Based on the signal loss in ventricular blood over time contrast washout occurred earlier than in volunteers. A hyperintense subendocardial rim was clearly visible in six patients (Fig. 5b) and barely detectable in another four. Four patients showed transmural lesions (Fig. 5c). LGE showed focal lesions in the one patient with senile amyloidosis. “Normal” appearance of LGE images with grey blood and dark myocardium

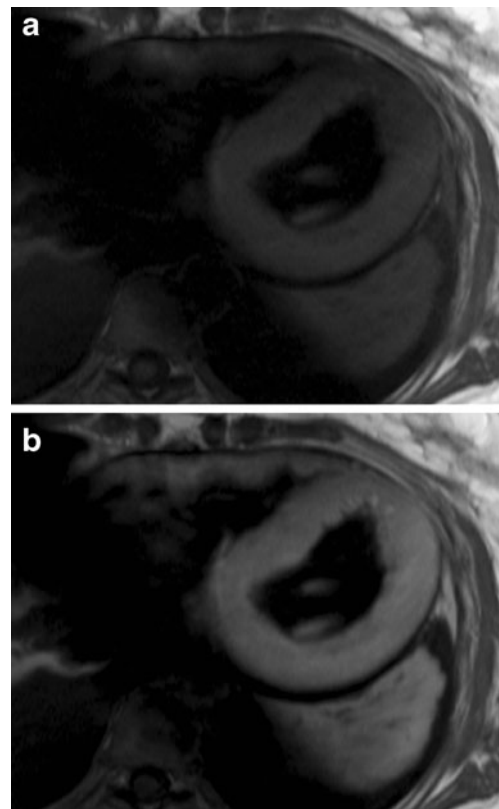


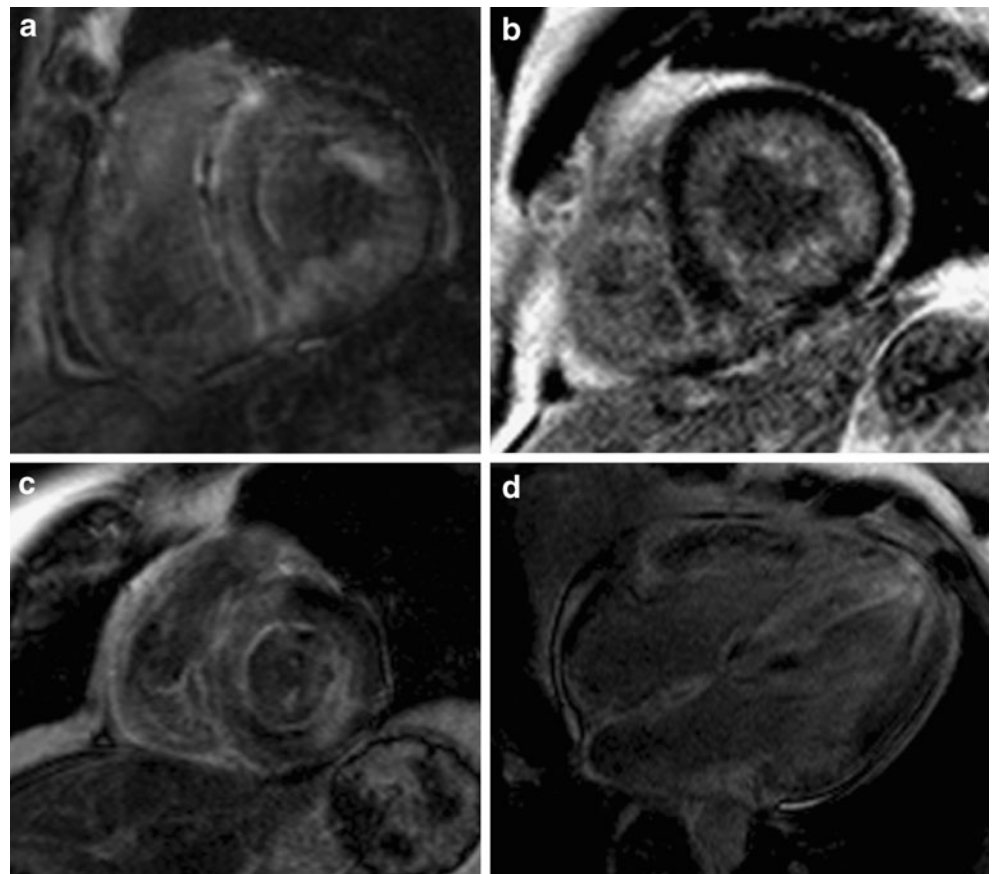
Fig. 4 Axial T1-weighted fast spin echo images before **a** and after **b** contrast medium administration indicate early myocardial contrast enhancement. An oblique saturation band is placed across the descending aorta to suppress flow artefacts

could be detected in one case only. In the remaining patients no focal lesions could be delineated, instead the myocardium could not be nulled, but appeared diffusely abnormal.

Atrial enhancement defined as bright atrial walls depicted with the late enhancement technique could be detected in 11 out of 31 patients (Fig. 5d).

Two cases with positive myocardial biopsy were missed on CMR: The first case was a patient with coronary artery disease and hypertension. Echocardiography revealed LV hypertrophy and suggested amyloidosis based on a sparkling pattern. CMR confirmed hypertrophy and delineated a small focal lesion on LGE images but could not detect evidence of amyloidosis. A biopsy taken during coronary revascularisation surgery was weakly positive in congo-red staining around small vessels only, suggesting senile amyloidosis rather than systemic or secondary amyloidosis. In the second case the patient had systemic AL amyloidosis, normal echocardiography and ECG, was not hypertrophic, did not have abnormal contrast medium uptake but did have a small pericardial effusion only. However, myocardial biopsy revealed amyloid infiltration.

Fig. 5 Late gadolinium enhancement inversion recovery fast low angle shot gradient echo images on the short axis (a-c) and 4CV (d). Enhancement pattern can be diffuse a, predominantly subendocardial b or transmural c, while the anterior wall is spared c. Involvement of the atrial septum is present in d



Discussion

Our results indicate that T2-weighted imaging may add diagnostic benefit in cardiac amyloidosis beyond unusual late enhancement patterns. Moreover this turned out to be of prognostic importance in our cohort (Fig. 6). On T2-weighted images we found decreased myocardial signal intensity compared with skeletal muscle. This is in accordance with T2-weighted imaging of extracardiac amyloid due to pronounced local field heterogeneity [24]

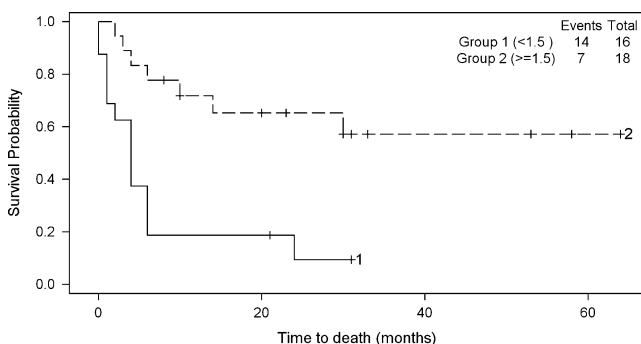


Fig. 6 Kaplan-Meier curves indicate shorter survival for patients with a T2 signal ratio below 1.5 (solid line) compared with those above 1.5 (dashed line)

and an early low-field CMR report of cardiac amyloidosis [25]. Our results do not yet allow a diagnosis of cardiac amyloidosis or a prognostic estimate based on T2 alone given the overlap between groups. In future studies it might be easier to assess the degree of amyloid infiltration based on changes in T2 contrast than based on LGE images that are difficult to quantify. Moreover T2-weighted imaging does not require contrast medium administration, which is of advantage in these patients with frequent renal failure.

Left ventricular hypertrophy, in the absence of other causes like arterial hypertension, is an established marker for cardiac amyloidosis [4]. Accordingly, marked LV hypertrophy was a frequent finding in our CMR study. However, more than a fourth of our patients did have normal wall thickness and LV mass.

Atrial enlargement is also frequently observed in cardiac amyloidosis as part of the restrictive haemodynamics, caused by increased stiffness of the LV. We could confirm mild left atrial enlargement in 56% of our patients using only biplanar measurements of the atrial area that might give a more accurate estimate of true atrial size than measurements of diameters alone [26]. Contrary to the findings in 16 patients in Bologna [27] the right atrial area was not markedly increased in our patients. Thickening of the atrial septum used to be a classical marker for

amyloidosis on echocardiography and early spin echo CMR studies [27]. In our study however, most atrial walls appeared to be of normal thickness as assessed by state of the art SSFP cine CMR with reduced blurring artefacts.

We found small pericardial effusions in almost all of our patients and pleural effusions in more than half of them, which reveals a higher sensitivity compared with older CMR reports and non-CMR series [6, 27, 28].

We found markedly increased early contrast medium uptake in almost all of our patients. Interestingly, enhancement was even higher and appeared more homogeneous than described before in patients with myocarditis [21]. In magnetic resonance studies of the tongue, amyloid infiltration resulted in considerably earlier contrast enhancement on T1-weighted images [29]. This rapid and pronounced contrast medium uptake is most likely due to an increase in interstitial space in the presence of amyloid infiltration [29].

Maceira et al. reported unusual gadolinium enhancement in amyloidosis with lower contrast between affected and remote myocardium compared with infarction or fibrosis [16]. Our study, as well as work from Perugini et al. [17] and case reports [30–32], confirm these findings. However, heterogeneous appearance on LGE images as a marker for amyloidosis appears problematic, as it is less striking and consistent than the enhancement patterns in infarction or in focal lesions of hypertrophic cardiomyopathy. Therefore it might be challenging to diagnose cardiac amyloidosis based on LGE imaging alone. Moreover the LGE pattern seems to be variable [33] with a homogeneously bright or exclusively subendocardial pattern in some patients [2, 32, 34–36]. We found subendocardial bright rims, elsewhere described as typical for amyloidosis [18, 36], in less than half of our cases. Therefore it appears challenging to quantify the extent of LGE in a standardised way. Within this study we did not attempt to quantify LGE for this reason. There are conflicting data regarding the prognostic impact of LGE [37, 38].

In cardiac amyloidosis Maceira et al. measured lower myocardial T1 values than in controls at 4 minutes after contrast [16]. This nicely matches our results with early contrast enhancement using a fast spin echo sequence. Therefore it seems important to underscore that their imaging approach was in fact not “late” and differed from conventional late enhancement imaging for infarction [10]. Depending on the imaging time after contrast enhancement the myocardial signal pattern is highly variable [32] and less stable than in myocardial infarction.

Atrial walls appeared bright in about a third of our patients confirming a case report by Lyne and coworkers [39]. Again, this was not a consistent pattern throughout the group.

Several limitations of our study have to be discussed. Not all of our patients underwent myocardial biopsy.

According to clinical guidelines [1, 40] the combination of extracardiac biopsy plus LV hypertrophy and low voltage ECG is clinically accepted as diagnostic even in the absence of myocardial biopsy. We did not quantify T1- or T2 relaxation times in this patient group, which might have elucidated more subtle differences in amyloid infiltration [41, 42]. While T1 or T2 measurement techniques are only research tools at the moment [43, 44], the aim of this study was to test a combination of widely available CMR imaging methods. The cause of death was assessed clinically by the referring clinician and not by autopsy.

In conclusion, cardiac amyloidosis is associated with hypointense myocardial signal on T2-weighted images. This might add diagnostic confidence beyond late gadolinium enhancement. Hypointense myocardium in T2 predicted short survival. We typically found small pericardial effusions, but not atrial wall thickening. Additional studies including direct quantification of T2 should further elucidate the relation between T2 signal and amyloid infiltration.

Acknowledgement We gratefully acknowledge the support of Carsten Schwenke (SCOSSiS Statistical Consulting). We sincerely thank Wilko Weichert MD, Pathology Institute, Charite, University Medicine Berlin, for providing Fig. 1. We are indebted to our technicians Denise Kleindienst, Kerstin Kretschel and Evi Polzin.

References

- Falk RH (2005) Diagnosis and management of the cardiac amyloidoses. *Circulation* 112:2047–2060
- Selvanayagam JB, Hawkins PN, Paul B, Myerson SG, Neubauer S (2007) Evaluation and management of the cardiac amyloidosis. *J Am Coll Cardiol* 50:2101–2110
- Roberts WC, Waller BF (1983) Cardiac amyloidosis causing cardiac dysfunction: analysis of 54 necropsy patients. *Am J Cardiol* 52:137–146
- Rahman JE, Helou EF, Gelzer-Bell R et al (2004) Noninvasive diagnosis of biopsy-proven cardiac amyloidosis. *J Am Coll Cardiol* 43:410–415
- Eriksson P, Backman C, Eriksson A, Eriksson S, Karp K, Olofsson BO (1987) Differentiation of cardiac amyloidosis and hypertrophic cardiomyopathy. A comparison of familial amyloidosis with polyneuropathy and hypertrophic cardiomyopathy by electrocardiography and echocardiography. *Acta Med Scand* 221:39–46
- Murtagh B, Hammill SC, Gertz MA, Kyle RA, Tajik AJ, Grogan M (2005) Electrocardiographic findings in primary systemic amyloidosis and biopsy-proven cardiac involvement. *Am J Cardiol* 95:535–537
- Kristen AV, Meyer FJ, Perz JB et al (2005) Risk stratification in cardiac amyloidosis: Novel approaches. *Transplantation* 80:S151–S155
- Nordlinger M, Magnani B, Skinner M, Falk RH (2005) Is elevated plasma b-natriuretic peptide in amyloidosis simply a function of the presence of heart failure? *Am J Cardiol* 96:982–984
- Dispenzieri A, Gertz MA, Kyle RA et al (2004) Serum cardiac troponins and n-terminal pro-brain natriuretic peptide: a staging system for primary systemic amyloidosis. *J Clin Oncol* 22:3751–3757

10. Kim RJ, Shah DJ, Judd RM (2003) How we perform delayed enhancement imaging. *J Cardiovasc Magn Reson* 5:505–514
11. Choudhury L, Mahrholdt H, Wagner A et al (2002) Myocardial scarring in asymptomatic or mildly symptomatic patients with hypertrophic cardiomyopathy. *J Am Coll Cardiol* 40:2156–2164
12. Moon JC, Reed E, Sheppard MN et al (2004) The histologic basis of late gadolinium enhancement cardiovascular magnetic resonance in hypertrophic cardiomyopathy. *J Am Coll Cardiol* 43:2260–2264
13. Hunold P, Schlosser T, Vogt FM et al (2005) Myocardial late enhancement in contrast-enhanced cardiac MRI: Distinction between infarction scar and non-infarction-related disease. *Am J Roentgenol* 184:1420–1426
14. Lim RP, Srichai MB, Lee VS (2007) Non-ischemic causes of delayed myocardial hyperenhancement on MRI. *Am J Roentgenol* 188:1675–1681
15. Bohl S, Wassmuth R, Abdel-Aty H et al (2008) Delayed enhancement cardiac magnetic resonance imaging reveals typical patterns of myocardial injury in patients with various forms of non-ischemic heart disease. *Int J Cardiovasc Imaging* 24:597–607
16. Maceira AM, Joshi J, Prasad SK et al (2005) Cardiovascular magnetic resonance in cardiac amyloidosis. *Circulation* 111:186–193
17. Perugini E, Rapezzi C, Piva T et al (2006) Noninvasive evaluation of the myocardial substrate of cardiac amyloidosis by gadolinium cardiac magnetic resonance. *Heart* 92(3):343–349
18. Vogelsberg H, Mahrholdt H, Deluigi CC et al (2008) Cardiovascular magnetic resonance in clinically suspected cardiac amyloidosis: Noninvasive imaging compared to endomyocardial biopsy. *J Am Coll Cardiol* 51:1022–1030
19. Seeger A, Klumpp B, Kramer U et al (2009) MRI assessment of cardiac amyloidosis: experience of six cases with review of the current literature. *Br J Radiol* 82:337–342
20. Abdel-Aty H, Boye P, Zagrosek A et al (2005) Diagnostic performance of cardiovascular magnetic resonance in patients with suspected acute myocarditis: comparison of different approaches. *J Am Coll Cardiol* 45:1815–1822
21. Friedrich MG, Strohm O, Schulz-Menger J, Marciniak H, Luft FC, Dietz R (1998) Contrast media-enhanced magnetic resonance imaging visualizes myocardial changes in the course of viral myocarditis. *Circulation* 97:1802–1809
22. Anderson JL, Horne BD, Pennell DJ (2005) Atrial dimensions in health and left ventricular disease using cardiovascular magnetic resonance. *J Cardiovasc Magn Reson* 7:671–675
23. Maceira AM, Prasad SK, Khan M, Pennell DJ (2006) Normalized left ventricular systolic and diastolic function by steady state free precession cardiovascular magnetic resonance. *J Cardiovasc Magn Reson* 8:417–426
24. Gean-Marton AD, Kirsch CF, Vezina LG, Weber AL (1991) Focal amyloidosis of the head and neck: evaluation with CT and MR imaging. *Radiology* 181:521–525
25. Celletti F, Fattori R, Napoli G et al (1999) Assessment of restrictive cardiomyopathy of amyloid or idiopathic etiology by magnetic resonance imaging. *Am J Cardiol* 83(798–801):a10
26. Barnes ME, Miyasaka Y, Seward JB et al (2004) Left atrial volume in the prediction of first ischemic stroke in an elderly cohort without atrial fibrillation. *Mayo Clin Proc* 79:1008–1014
27. Fattori R, Rocchi G, Celletti F, Bertaccini P, Rapezzi C, Gavelli G (1998) Contribution of magnetic resonance imaging in the differential diagnosis of cardiac amyloidosis and symmetric hypertrophic cardiomyopathy. *Am Heart J* 136:824–830
28. Berk JL (2005) Pleural effusions in systemic amyloidosis. *Curr Opin Pulm Med* 11:324–328
29. Asaumi J, Yanagi Y, Hisatomi M, Konouchi H, Kishi K (2001) CT and MR imaging of localized amyloidosis. *Eur J Radiol* 39:83–87
30. Sueyoshi E, Sakamoto I, Okimoto T, Hayashi K, Tanaka K, Toda G (2006) Cardiac amyloidosis: typical imaging findings and diffuse myocardial damage demonstrated by delayed contrast-enhanced MRI. *Cardiovasc Intervent Radiol* 29:710–712
31. vanden Driesen RI, Slaughter RE, Struggnell WE (2006) MR findings in cardiac amyloidosis. *AJR Am J Roentgenol* 186:1682–1685
32. Bucciarelli-Ducci C, Locca D, Barbeau G, Prasad SK (2007) Value of cardiovascular magnetic resonance for determining cardiac involvement in systemic amyloidosis. *Eur Heart J* 28:1186
33. Syed IS, Glockner JF, Feng D et al (2010) Role of cardiac magnetic resonance imaging in the detection of cardiac amyloidosis. *JACC Cardiovasc Imaging* 3:155–164
34. Leeson CP, Myerson SG, Walls GB, Neubauer S, Ormerod OJ (2006) Atrial pathology in cardiac amyloidosis: evidence from ECG and cardiovascular magnetic resonance. *Eur Heart J* 27:1670
35. Van Geluwe F, Dymarkowski S, Crevits I, De Wever W, Bogaert J (2006) Amyloidosis of the heart and respiratory system. *Eur Radiol* 16:2358–2365
36. Cheng AS, Banning AP, Mitchell AR, Neubauer S, Selvanayagam JB (2006) Cardiac changes in systemic amyloidosis: visualisation by magnetic resonance imaging. *Int J Cardiol* 113:E21–E23
37. Ruberg FL, Appelbaum E, Davidoff R et al (2009) Diagnostic and prognostic utility of cardiovascular magnetic resonance imaging in light-chain cardiac amyloidosis. *Am J Cardiol* 103:544–549
38. Austin BA, Tang WH, Rodriguez ER et al (2009) Delayed hyperenhancement magnetic resonance imaging provides incremental diagnostic and prognostic utility in suspected cardiac amyloidosis. *JACC Cardiovasc Imaging* 2:1369–1377
39. Lyne JC, Petryka J, Pennell DJ (2008) Atrial enhancement by cardiovascular magnetic resonance in cardiac amyloidosis. *Eur Heart J* 29:212
40. Gertz MA, Comenzo R, Falk RH et al (2005) Definition of organ involvement and treatment response in immunoglobulin light chain amyloidosis (al): a consensus opinion from the 10th international symposium on amyloid and amyloidosis, Tours, France, 18–22 April 2004. *Am J Hematol* 79:319–328
41. Maceira AM, Prasad SK, Hawkins PN, Roughton M, Pennell DJ (2008) Cardiovascular magnetic resonance and prognosis in cardiac amyloidosis. *J Cardiovasc Magn Reson* 10:54
42. Sparrow P, Amirabadi A, Sussman MS, Paul N, Merchant N (2009) Quantitative assessment of myocardial T2 relaxation times in cardiac amyloidosis. *J Magn Reson Imaging* 30:942–946
43. Krombach GA, Hahn C, Tomars M et al (2007) Cardiac amyloidosis: MR imaging findings and T1 quantification, comparison with control subjects. *J Magn Reson Imaging* 25:1283–1287
44. Hosch W, Bock M, Libicher M et al (2007) MR-relaxometry of myocardial tissue: significant elevation of T1 and T2 relaxation times in cardiac amyloidosis. *Invest Radiol* 42:636–642